A planar left-handed metamaterial based on electric resonators*

Chen Chun-Hui(陈春晖)[a)†], Qu Shao-Bo(屈绍波)[a)b)‡], Wang Jia-Fu(王甲富)[a)], Ma Hua(马 华)[a)], Wang Xin-Hua(王新华)[a)], and Xu Zhuo(徐 卓)[b)]

[a)] *College of Science, Air Force Engineering University, Xi'an* 710051, *China*

[b)] *Electronic Materials Research Laboratory, Key Laboratory of the Ministry of Education, Xi'an Jiaotong University, Xi'an* 710049, *China*

(Received 26 June 2010; revised manuscript received 29 November 2010)

A planar left-handed metamaterial(LHM) composed of electric resonator pairs is presented in this paper. Theoretical analysis, an equivalent circuit model and simulated results of a wedge sample show that this material exhibits a negative refraction pass-band around 9.6GHz under normal-incidence and is insensitive to a change in incidence angle. Furthermore, as the angle between the arm of the electric resonators and the strip connecting the arms increases, the frequency range of the pass-band shifts downwards. Consequently, this LHM guarantees a relatively stable torlerence of errors when it is practically fabricated. Moreover, it is a candidate for designing multi-band LHM through combining the resonator pairs with different angles.

Keywords: planar left-handed metamaterial, electric resonator, multi-band metamaterial

PACS: 41.20.Jb, 42.25.Bs, 73.20.Mf, 77.22.Ch **DOI:** 10.1088/1674-1056/20/3/034101

1. Introduction

Left-handed metamaterials (LHMs) that possess a negative refractive index have been extensively studied in the past decade for their special physical properties[1] and applications in diverse domains such as the design of perfect lens[2] and cloaking devices.[3] Nowadays, various configurations have been created and fabricated, such as the S-shaped structure[4] and the fishnet structure.[5]

Based on the Pendry method*et al.*, the first LHM[6] was numerically and experimentally demonstrated in a microwave regime in 2000 and was composed of non-resonant continuous wires[7] and split-ring resonators (SRRs).[8] According to this principle, the Soukoulis group fabricated a bulk composite metamaterial that realized a negative refractive index at 100 GHz.[9] However, it is not advisable to use continuous wires to construct finite and contoured objects such as cloaking devices.[10,11] Then, with the aim of surmounting limitations in their practical application, Schurig *et al.* designed electric resonators in the microwave frequency range as alternatives to wire media.[12] Alexander *et al.* studied the electric response of the resonators over the THz range.[13] Yuan *et al.* modified previous structures and fabricated a dual resonant electric resonator at THz.[14] The electric resonators provided another route for the design of LHMs. Later, through combining the SRRs and electric resonators, and tuning their geometrical parameters to make them resonate at the same frequency range, an impedance-matching and relatively broadband LHM was experimentally realized by Liu *et al.*[15] Wang *et al.* constructed multi-band LHMs[16] by placing electric resonators in the centre space of the SRRs. When combining electric and magnetic resonators, it is necessary to adjust the geometric dimensions of the structures to make the two resonant frequency ranges overlap. Meanwhile, when plane waves propagate in the LHM, the electric resonance frequency will be modified by the SRRs providing an electric response as short wires along the direction of the electric field.

Among previous LHMs, the electric resonators were merely used to produce $\varepsilon < 0$. Considering the former disadvantages, in this paper, we propose another method to realize a LHM composed of electric resonator pairs. By means of setting up an equivalent circuit model, numerical analysis and simulating the

*Project supported by the National Natural Science Foundation of China (Grant Nos. 50632030 and 60871027), the National Basic Research Program of China(Grant No. 2009CB613306) and the Natural Science Foundation of Shaanxi Province, China (Grant No. SJ08F01).

†E-mail: baoercherry@yahoo.com.cn

‡Corresponding author. E-mail: qushaobo@mail.xjtu.edu.cn

© 2011 Chinese Physical Society and IOP Publishing Ltd

wedge sample, we confirm that this planar metamaterial exhibits a negative refraction pass-band. We also discuss the influences of the incidence angle and the angle between the arm of the electric resonators and the strip connecting the arms.

2. Structure model and equivalent LC circuit analysis

The unit cell of a typical fishnet structure[13] is depicted in Fig. 1(a). We altered the direction of the parallel wires to form electric resonator pairs. Figure 1(b) shows the unit cell of the material we designed. Identical copper ($\sigma = 5.8 \times 10^7$ S/m) patterns (strip thickness $d_1 = 0.017$ mm) are etched on both sides of a FR-4 substrate ($\varepsilon_r = 4.6$, $\tan\delta = 0.0004$). The copper patterns are identical on both sides of the substrate.

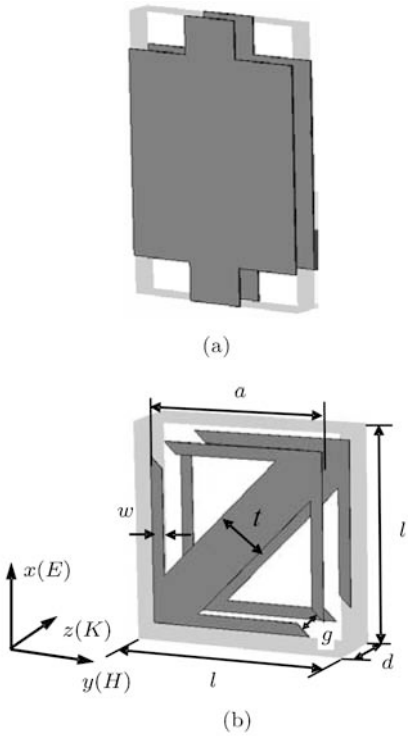


Fig. 1. (a) The unit cell of the fishnet structure, (b) the unit cell of the electric resonator pairs structure with the geometric dimensions $l = 9.0$ mm, $a = 7.5$ mm, $g = 0.9$ mm, $d = 2.7$ mm, $t = 2.1$ mm and $w = 0.5$ mm.

To analyse whether this electric resonator pairs structure could present left-handed behavior in a certain frequency range, we set up an equivalent LC circuit model for both magnetic and electric responses. The electric resonators on each side of the substrate form an electric resonance LC circuit. The equivalent circuit can be described by Fig. 2(a), where L_1 is the effective inductance of the strip connecting the arms of the electric resonators, L_2 is the effective inductance of the arms, C_g is the effective capacitance between the two arms. Under normal incidence, there are two induced circuit currents flowing in opposite directions in the structure because of its symmetry. The electric resonant frequency can be obtained by $f_e = 1/2\pi\sqrt{L_e C_e}$. The total inductance of the electric resonators can be obtained by $L_e = L_1 L_2/(L_1 + L_2)$. L_1 and L_2 can be approximated by

$$L_1 \approx \frac{\mu_0 c}{\pi} \ln\left(\frac{6.6c}{t + d_1}\right), \tag{1}$$

$$L_2 \approx \frac{\mu_0 b}{\pi} \ln\left(\frac{6.6b}{w + d_1}\right), \tag{2}$$

where c is the effective length of the strip, b is the length of the electric resonator arm and A is the modifying coefficient.[17] The capacitance is

$$C_e = 2C_g \sim \varepsilon_0 \varepsilon_r' \frac{w d_1}{g}, \tag{3}$$

where ε_r' is the relative permittivity, which is the ratio of the permittivity of the substrate to that of free space and g is the distance between the two arms. Therefore,

$$f_e = \frac{1}{2\pi\sqrt{L_e C_e}} \sim A' \frac{t w d_1}{a b} \cdot \frac{1}{\sqrt{C_e}}, \tag{4}$$

where A' is the modifying factor.

The magnetic resonance mainly originates from couplings between the strips connecting the arms of the electric resonator on both sides of the substrate. When the electromagnetic waves are normally incident, there is an induced current loop along the z direction to form an effective resonant circuit, as shown in Fig. 2(b). C_s is the effective capacitance between the two parallel strips on both sides of the substrate. The magnetic resonance frequency can be described as $f_m = 1/2\pi\sqrt{L_m C_m}$, where $L_m = L_e$ and $C_m = 2C_s + 2C_g$. As a result,

$$f_m = \frac{1}{2\pi\sqrt{L_m C_m}} \sim B' \frac{t w d_1}{a b} \cdot \frac{1}{\sqrt{C_m}}, \tag{5}$$

B' is the modifying factor and

$$C_m \sim B \varepsilon_0 \varepsilon_r' \frac{S}{d}, \tag{6}$$

where S is the area of the electric resonators.

According to the above analysis, the electric and magnetic resonant frequencies are affected by the geometric dimensions of the electric resonators and the substrates. By optimized design, there will be a LHM composed of electric resonator pairs as expected.

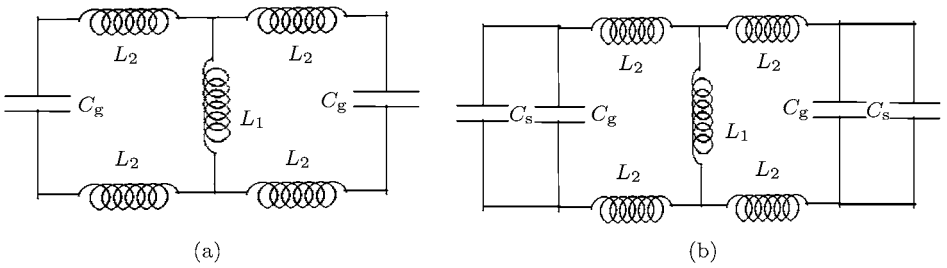


Fig. 2. The equivalent circuits for electric resonance (a) and magnetic resonance (b).

3. Left-handed properties of the electric resonator pairs metamaterial

At first, we simulated the electric resonator structure on a single side of the substrate, as shown in Fig. 1(b). In the normal-incidence case, we took the wave vector perpendicular to the substrate and fixed the polarization of electric vector and magnetic vector along the x and y direction, respectively. Figure 3 shows the simulated transmission spectra, in which there is an electric resonance around 9.0–10.4 GHz. According to the analysis in the previous section, it is an electric resonant stop-band and we will also analyse this electric resonance in this part. To demonstrate the left-handed properties of this electric resonator pairs structure, we simulated the transmission in one unit cell with periodic boundary conditions. The simulated transmission result is shown in Fig. 4. From Fig. 4, we find a pass-band in the frequency range around 9.1–10.0 GHz, which is a stop-band in Fig. 3. The difference between Figs. 3 and 4 4 demonstrates plane wave propagation through the material. Figure 5 shows the distribution of the induced currents on the two sides of the structure, in which the arrows represent the orientations of the induced currents. From Fig. 5, we find that the orientation of the current on side (a) is opposite to that of the current on side (b), forming a magnetic dipole moment parallel to the substrate. This is consistent with the theoretical analysis in section 2. Meanwhile, from the electric field distribution in Fig. 6, it can be confirmed that there is an electric dipole moment along the direction of the electric field. Both of them simultaneously form the foundations of electric and magnetic resonance. Thus, we predict that the pass-band around 9.1–10.0 GHz shown in Fig. 4 is a negative refraction pass-band.

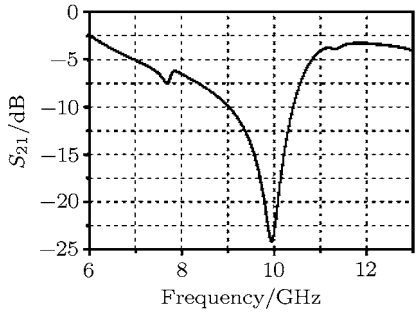


Fig. 3. Simulated transmission spectrum of the single electric resonator under normal incidence.

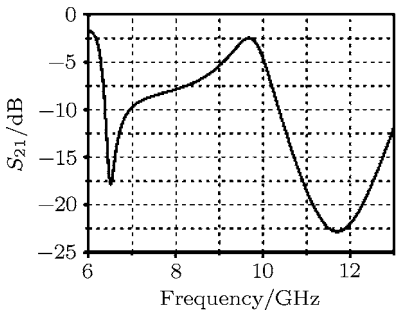


Fig. 4. Simulated transmission spectrum of the electric resonator pairs under normal incidence.

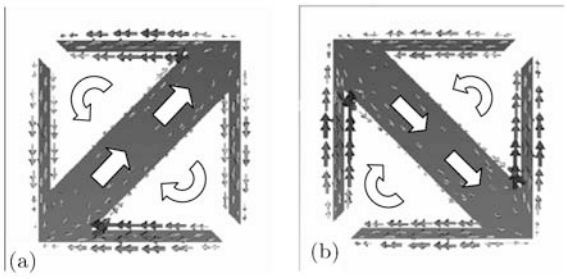


Fig. 5. Distribution of the induced currents in the copper wires on side (a) and on side (b) at 9.6 GHz.

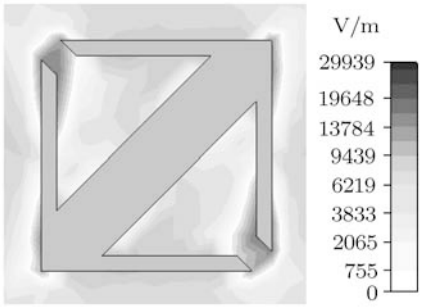


Fig. 6. Distribution of the electric field at 9.6 GHz.

To further verify the negative refraction of the electric resonator pairs metamaterial, we carried out the wedge sample simulation. The wedge sample was composed of 15×16 unit cells of electric resonator pairs structure in y and z directions, respectively. The boundary conditions along the x direction were perfect electric conditions (PEC). The simulated results are shown in Fig. 7, in which the arrows indicate the propagation directions of the refracted wave. From Fig. 7(a), there is a positive refraction at 8.7 GHz and the refraction angle was about 19 degrees. Compared with Figs. 7(a), 7(b) shows that there is a negative refraction at 9.9 GHz with a negative refractive angle of around −23 degrees. Corresponding to the pass-band in Fig. 4, we could be sure that it is a left-handed pass-band in the frequency range of 9.1–10.0 GHz.

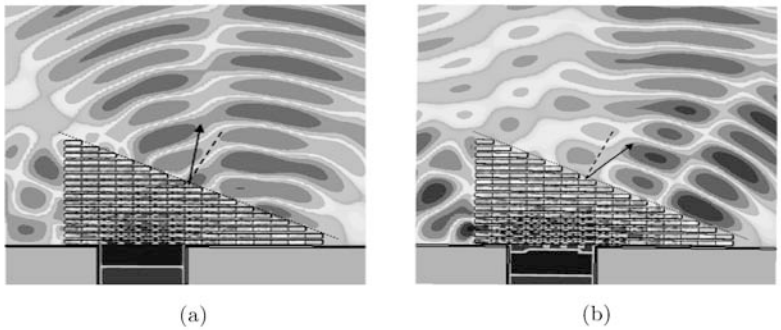


Fig. 7. Positive and negative refractions of the wedge sample at 8.7 GHz (a) and 9.9 GHz (b).

4. Discussion of changing the incidence angle and rotating the arms

4.1. Influences of the incidence angle

In order to investigate the influence of the incidence angle θ, we simulated with different wave vectors k, as shown in Fig. 8(a), while keeping the polarization direction unchanged. Figure 8(b) is the simulated transmission line when the incidence angle was 15°, 30° and 45°, respectively. In Fig. 8(b), there is minor blue-shift for the transmission peak as the incidence angle θ increases. When the incidence angle changes, the direction of the magnetic field changes correspondingly while the polarization direction keeps unchanged. From the analysis in Section 3, we confirmed that the currents in the electric resonators structure were mainly induced by the electric field. As a result, this structure is insensitive to the change of the incidence angle.

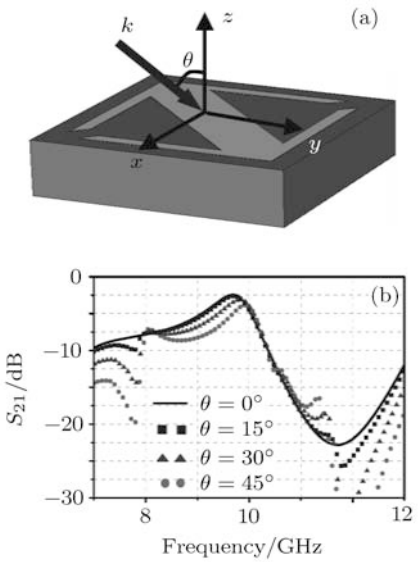


Fig. 8. (a) Illustration of the incident plane wave with wave vector k and incidence angle θ, (b) simulated transmission spectra of the electric resonator pairs structure when the incidence angle θ is changed.

4.2. Influences of rotating the arms of the electric resonators

We designed the electric resonator pairs metamaterial by altering the direction of the cut wires in the fishnet structure. To explore the relationship between the rotated angle i and the resonant frequency range, we tuned the length of the arms as well as the angle i between the arm and the strip by five degrees when the dimensions of the structure and the distance between the arms remained unchanged, as shown in Figs. 9(a) and 9(b).

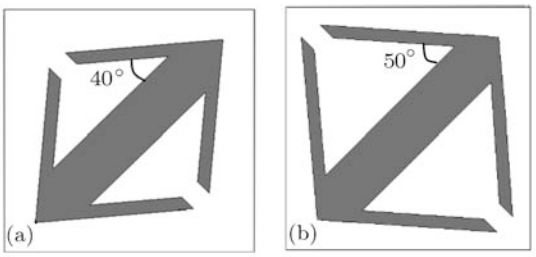


Fig. 9. The modified structure by tuning the angle for $-5°$ (a) and $5°$ (b).

Figure 10 gives the dependence of the transmission results on the angle i. The resonant frequency range shifts downwards as the angle increases. This can be explained by Eqs. (4) and (5). When the angle is 50°, to keep the distance between the arms unchanged, the length b increases leading to larger $L_{\rm m}$ and $L_{\rm e}$. Consequently, the resonant frequency becomes lower than the case when the angles are 45° and 40°. Meanwhile, in Fig. 10, there is always a left-handed pass-band for different angles, indicating that this structure had a relatively stable tolerance of errors in practical fabrication.

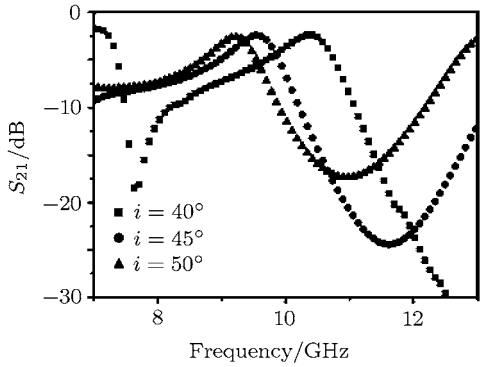


Fig. 10. Simulated transmission results for the angle $i = 40°$, 45° and 50°.

It is also a candidate for multi-band LHMs. As examples, two typical structures were presented through arranging arrays of unit cells with angle $i = 40°$ and 50° in two ways as shown in Figs. 11(a) and 12(a), respectively. Figure 11(b) shows the simulated transmission parametersS_{11} and S_{21} of the structure arranged in the first way. Comparing Figs. 10 and 11(b), we find that the two transmission peaks of the combined structure are almost the same as the ones in Fig. 10. In addition, Fig. 12(b) gives the simulated transmission parameters S_{11} and S_{21} when combining the unit cells in the second way. In Fig. 12(b), we find two transmission peaks at 9.5 and 10.8 GHz, respectively, which are almost consistent with the passbands in Fig. 10. Both two combined structures possess two left-handed passbands. The minor reductions of transmission and the neglectable blue-shifts for the transmission peaks in both Figs. 11(b) and 12(b) mainly originate from the slightly increased resonant frequencies and the couplings between the unit cells.

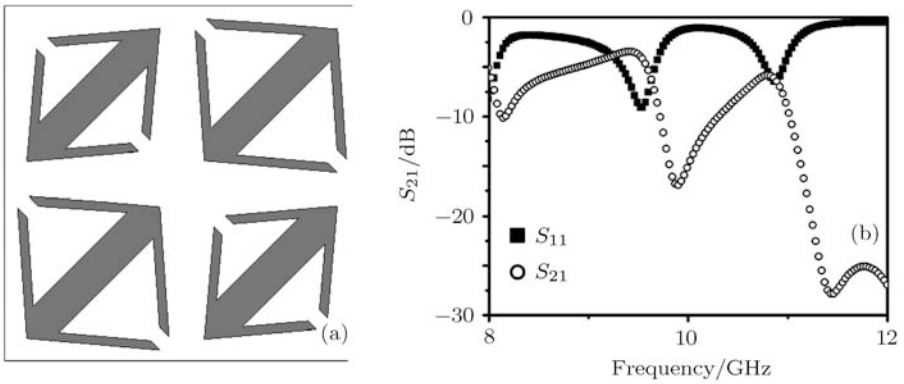


Fig. 11. (a) The multi-band LHMs arranged in the first way, (b) the simulated transmission parameters S_{11} and S_{21}.

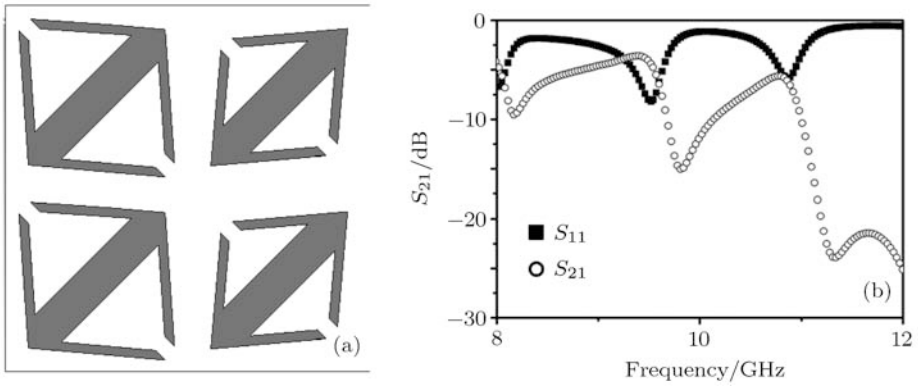


Fig. 12. (a) The multi-band LHMs arranged in the second way, (b) the simulated transmission parameters S_{11} and S_{21}.

5. Conclusion

In conclusion, our work has clarified the possibility of designing LHM based on electric resonator pairs. Theoretical analysis, an equivalent circuit model and simulated results indicate that this electric resonator pairs metamaterial simultaneously exhibits negative effective permittivity and permeability in the frequency range around 9.1–10.0 GHz. Meanwhile, this structure is independent of the incidence angle. Furthermore, the frequency range of the negative refractive pass-band shifts downwards as the angle between the arm and the strip of the electric resonators increases. Thus, this structure guarantees a relatively stable tolerance of errors in practical fabrication. It is also a potential candidate for constructing multi-band LHMs when the electric resonator pairs with different angles are combined.

References

[1] Veselago V G 1968 *Sov. Phys. Usp.* **10** 509
[2] Fang N, Lee H, Sun C and Zhang X 2005 *Science* **308** 534
[3] Pendry J B, Schurig D and Smith D R 2006 *Science* **312** 1780
[4] Chen H S, Ran L X, Huangfu J T Zhang X M, Chen K S, Grzegorczyk T M and Kong J A 2007 *Phys. Rev.* B **76** 024402
[5] Alici K B and Ozbay E 2008 *Photon. Nanostruct.: Fundam. Applic.* **6** 102
[6] Shelby R A, Smith D R and Schultz S 2001 *Science* **292** 77
[7] Pendry J B, Holden A J, Stewart W J and Youngs I 1996 *Phys. Rev. Lett.* **76** 4773
[8] Pendry J B, Holden A J, Robbins D J and Stewart W J 1999 *IEEE Trans. Microwave Theor. Techniq.* **47** 2075
[9] Gokkavas M, Guven K, Bulu I, Aydin K, Penciu R S, Kafesaki M, Soukoulis C M and Ozbay E 2006 *Phys. Rev.* B **73** 13103
[10] Ma H, Qu S B, Xu Z, Zhang J Q and Wang J F 2009 *Chin. Phys.* B **18** 1025
[11] Ma H, Qu S B, Xu Z and Wang J F 2009 *Chin. Phys.* B **18** 1123
[12] Schurig D, Mock J J and Smith D R 2007 *Appl. Phys. Lett.* **90** 263504
[13] Alexander M, Dragomir N N, David A P, Ilya V S, Mikhail L, Ian M, Haroldo T H, Hark H T, Chennupati J and Yuri S K 2010 *Phys. Rev.* B **81** 115109
[14] Yuan Y, Bingham C, Tyler T, Palit S, Hand T H, Padilla W J, Jokerst N M and Cummer S A 2008 *Appl. Phys. Lett.* **93** 191110
[15] Liu R P, Degiron A, Mock J J and Smith D R 2007 *Appl. Phys. Lett.* **90** 263504
[16] Wang J F, Qu S B, Yang Y M, Ma H, Wu X and Xu Z 2009 *Appl. Phys. Lett.* **95** 014105
[17] Bahl I, and Bhartia P 2003 *Microwave Solid State Circuit Design* (New Jersey: John Wiley & Sons)